Clinical and electrophysiological features of *SCN8A* variants causing episodic or chronic ataxia

Hang Lyu,[a,u] Christian M. Boßelmann,[a,u] Katrine M. Johannesen,[b,c] Mahmoud Koko,[a] Juan Dario Ortigoza-Escobar,[d] Sergio Aguilera-Albesa,[e,t] Deyanira Garcia-Navas Núñez,[f] Tarja Linnankivi,[g] Eija Gaily,[g] Henriette J. A. van Ruiten,[h] Ruth Richardson,[i] Cornelia Betzler,[j,k] Gabriella Horvath,[l] Eva Brilstra,[m] Niels Geerdink,[n] Daniele Orsucci,[o] Alessandra Tessa,[p] Elena Gardella,[c,q] Zofia Fleszar,[r,s] Ludger Schöls,[r,s] Holger Lerche,[a] Rikke S. Møller,[c,q] and Yuanyuan Liu[a,*]

[a]Department of Neurology and Epileptology, Hertie Institute for Clinical Brain Research, University of Tuebingen, Tuebingen, Germany
[b]Department of Clinical Genetics, University Hospital of Copenhagen, Rigshospitalet, Copenhagen, Denmark
[c]Department of Epilepsy Genetics and Personalized Medicine, The Danish Epilepsy Centre (Member of the ERN EpiCARE), Dianalund, Denmark
[d]Movement Disorders Unit, Institut de Recerca Sant Joan de Déu, CIBERER-ISCIII and European Reference Network for Rare Neurological Diseases (ERN-RND), Barcelona, Spain
[e]Pediatric Neurology Unit, Department of Pediatrics, Hospital Universitario de Navarra, Pamplona, Spain
[f]Pediatrics Department, San Pedro de Alcántara Hospital, Cáceres, Spain
[g]Department of Pediatric Neurology, New Children's Hospital and Pediatric Research Center, Epilepsia Helsinki, Helsinki University Hospital and University of Helsinki, Helsinki, Finland
[h]Newcastle Upon Tyne Hospitals NHS Foundation Trust, Great North Children's Hospital, Newcastle upon Tyne, UK
[i]Northern Genetics Service, The Newcastle Upon Tyne Hospitals NHS Foundation Trust, UK
[j]Institute for Rehabilitation, Transition and Palliation, Paracelsus Medical University, Salzburg, Austria
[k]Specialist Center for Paediatric Neurology, Neuro-Rehabilitation and Epileptology, Schön Klinik Vogtareuth, Germany
[l]Adult Metabolic Diseases Clinic, BC Children's Hospital, Vancouver, Canada
[m]Department of Genetics, University Medical Center Utrecht, Utrecht, the Netherlands
[n]Department of Pediatrics, Rijnstate Hospital, Arnhem, the Netherlands
[o]Unit of Neurology, San Luca Hospital, Lucca, Italy
[p]IRCCS Stella Maris Foundation, Calambrone, Pisa, Italy
[q]Department of Regional Health Research, Faculty of Health Sciences, University of Southern Denmark, Denmark
[r]Department of Neurodegenerative Diseases, Hertie Institute for Clinical Brain Research, University of Tuebingen, Tuebingen, Germany
[s]German Center for Neurodegenerative Diseases (DZNE), Tübingen, Germany
[t]Navarrabiomed-Fundación Miguel Servet, Pamplona, Spain

Summary

Background Variants in *SCN8A* are associated with a spectrum of epilepsies and neurodevelopmental disorders. Ataxia as a predominant symptom of *SCN8A* variation has not been well studied. We set out to investigate disease mechanisms and genotype–phenotype correlations of *SCN8A*-related ataxia.

Methods We collected genetic and electro-clinical data of ten individuals from nine unrelated families carrying novel *SCN8A* variants associated with chronic progressive or episodic ataxia. Electrophysiological characterizations of these variants were performed in ND7/23 cells and cultured neurons.

Findings Variants associated with chronic progressive ataxia either decreased Na^+ current densities and shifted activation curves towards more depolarized potentials (p.Asn995Asp, p.Lys1498Glu and p.Trp1266Cys) or resulted in a premature stop codon (p.Trp937Ter). Three variants (p.Arg847Gln and biallelic p.Arg191Trp/p.Asp1525Tyr) were associated with episodic ataxia causing loss-of-function by decreasing Na^+ current densities or a hyperpolarizing shift of the inactivation curve. Two additional episodic ataxia-associated variants caused mixed gain- and loss-of function effects in ND7/23 cells and were further examined in primary murine hippocampal neuronal cultures. Neuronal firing in excitatory neurons was increased by p.Arg1629His, but decreased by p.Glu1201Lys. Neuronal firing in inhibitory neurons was decreased for both variants. No functional effect was observed for p.Arg1913Trp. In four individuals, treatment with sodium channel blockers exacerbated symptoms.

eBioMedicine
2023;98: 104855
Published Online xxx
https://doi.org/10.1016/j.ebiom.2023.104855

*Corresponding author. Department of Neurology and Epileptology, Hertie Institute for Clinical Brain Research, University of Tuebingen, Otfried-Mueller-Str. 27, D-72076, Tuebingen. Germany.
E-mail address: yuanyuan.liu@uni-tuebingen.de (Y. Liu).
[u]These authors contributed equally to this work.

Interpretation We identified episodic or chronic ataxia as predominant phenotypes caused by variants in *SCN8A*. Genotype-phenotype correlations revealed a more pronounced loss-of-function effect for variants causing chronic ataxia. Sodium channel blockers should be avoided under these conditions.

Funding BMBF, DFG, the Italian Ministry of Health, University of Tuebingen.

Keywords: *SCN8A*; Chronic ataxia; Episodic ataxia; Loss-of-function; Patch-clamp

Research in context

Evidence before this study

Variants in *SCN8A*, a gene encoding the voltage-gated sodium channel $Na_V1.6$, have been associated with neurodevelopmental disorders, including epilepsy, intellectual disability, and autism spectrum disorder. Ataxia-predominant phenotypes, where ataxia is the primary feature and neurodevelopmental abnormalities are mild or absent, and episodic ataxia were not previously considered part of the clinical spectrum of *SCN8A*-related disorder, and their mechanism was not well-understood.

Added value of this study

In this study, we establish episodic or predominant chronic ataxia as syndromes caused by de novo and familial missense variants or haploinsufficiency in *SCN8A*. In ND7/23 and hippocampal neurons, each missense variant resulted in an overall $Na_V1.6$ channel loss-of-function. We identified genotype–phenotype correlations that explain how differential functional effects at the molecular and neuronal level influence ataxia type, disease severity, and treatment response.

Implications of all the available evidence

Loss-of-function *SCN8A* variants may represent an underdiagnosed aetiology in hereditary ataxia. Treatment with sodium channel blockers, commonly prescribed in other types of episodic ataxia, may harm these individuals, and should be avoided. These implications provide valuable insights for clinicians in diagnosing and managing individuals affected by *SCN8A*-associated ataxia.

Introduction

Ataxia denotes a clinical syndrome of incoordination caused by cerebellar dysfunction.[1] In hereditary chronic ataxia, gait ataxia is a common initial symptom at disease onset, with postural instability, intention tremor, dysdiadochokinesia, cerebellar dysarthria, oculomotor dysfunction, and a wide range of other symptoms presenting as ataxia-plus syndromes.[2] In primary episodic ataxia, both cerebellar dysfunction and non-ataxia symptoms (including migraine, brainstem and cortical signs) occur in attacks of variable duration and frequency, while interictal symptoms are less pronounced or absent.[3] Chronic or episodic ataxia are primarily genetic disorders, and genetic testing can establish a diagnosis in up to two thirds of cases.[4]

Ion channel variants are involved in hereditary ataxia, epilepsy, paroxysmal movement disorder, peripheral nerve hyperexcitability, and other neurological disorders.[5,6] The human gene *SCN8A* encodes the voltage-gated sodium channel $Na_V1.6$, which is essential for the initiation and propagation of action potentials and is broadly expressed in the brain, particularly in the cerebellum.[6,7] Our previous studies have shown that *SCN8A* variants causing gain-of-function (GOF) are mainly associated with self-limiting or intermediate forms of focal epilepsy, and particularly with severe developmental and epileptic encephalopathies. Conversely, loss-of-function (LOF) variants are related to generalised epilepsy and neurodevelopmental disorders without epilepsy.[8,9] While the neurodevelopmental and epilepsy phenotype of *SCN8A* is well established, the spectrum of *SCN8A*-associated movement disorders is less well understood and *SCN8A* variants may represent an underdiagnosed aetiology of hereditary ataxia.

Missense variants in genes encoding neuronal voltage-gated cation channels are commonly associated with ataxia.[5,10–14] Through functional studies, we can delineate their distinct disease mechanisms and more clearly define the mechanisms of variants causing predominantly ataxia, contributing towards both a timely and accurate diagnosis as well as precision medicine approaches for individuals affected by these variants: In *SCN2A*- and *SCN8A*-associated epilepsy, treatment with sodium channel blockers (SCBs) has been shown to be beneficial in GOF-variant carriers, but unfavourable in those carrying LOF variants.[8,15] It is currently unclear if this extends to the treatment of other symptoms than seizures.

In this study, we recruited ten individuals from nine unrelated families with hereditary episodic or chronic ataxia associated with likely disease-causing variants in *SCN8A*. We characterised the biophysical effects of missense variants in heterologous and neuronal

expression systems. We found differential functional mechanisms to be closely correlated with clinical features including disease severity and type of ataxia. Our results establish causal evidence for *SCN8A*-associated episodic and chronic ataxia.

Methods

Recruitment and clinical data collection

Study participants with chronic or episodic ataxia as a predominant symptom and (likely) pathogenic variants or variants of unknown significance in *SCN8A* (detected by genetic testing using panel or whole exome sequencing) were recruited through an international network of clinicians. We used standardised phenotyping sheets to retrospectively collect pseudonymized demographic, clinical, electrographic, and imaging features. Where applicable, clinical features were harmonised with human phenotype ontology (HPO) terms, release v2022-06-11.[16]

Ethics

Informed consent was obtained from all individuals and/or caregivers, and all clinical procedures and genetic testing, including data collection and report, were in accordance with the declaration of Helsinki and approved by the local ethical committees or followed other local guidelines. Animal protocols for the generation of primary neuronal cultures were approved by the local Animal Care and Use Committee (Regierungspraesidium Tuebingen).

Mutagenesis

Mutagenesis was performed as previously described, the human $Na_V1.6$ channel α-subunit (Origene, PS100007) was modified to be tetrodotoxin (TTX, a neurotoxin blocking Na_V channels in nerve cells) insensitive by introducing a point mutation (c.1112 A > G, p.Y371C).[17] Ataxia-related *SCN8A* variants were engineered into this TTX-resistant $Na_V1.6$ channel construct using Pfu polymerase (Promega; primers are available upon request). Wild-type (WT) or mutant cDNA was fully sequenced before use to exclude any additional sequence alterations.

Cell culture and transfections

WT or mutant *SCN8A* cDNA together with human β1- and β2-subunits of voltage-gated Na^+ channels (pCLH-hβ1-EGFP and pCLH-hβ2-CD8) were transfected into ND7/23 cells (Sigma–Aldrich, RRID:CVCL_4259; cells were used at low passages, and recent mycoplasma testing has been performed) as previously described.[17] Electrophysiological recordings were performed 48 h after transfection and only from cells with TTX-resistant Na^+ current that tested positive for both anti-CD8 antibody coated microbeads and green fluorescence to be sure that both β1-and β2-subunits are co-expressed. Hippocampal neurons were obtained as previously described.[17] WT or mutant human *SCN8A* cDNA (1 μg) together with cDNA encoding GFP (0.1 μg) under the promoter targeting either excitatory or inhibitory neurons (Addgene; pAAV-CAMKII-GFP, plasmid #64545; pAAV-mDlx-GFP-Fishell-1, plasmid #83900) were transfected into neurons following the standard protocol of Optifect (Invitrogen). After 48 h, electrophysiological recordings were performed from fluorescence-positive neurons. For functional investigations employing ND7/23 cells or primary hippocampal neuronal cultures, the sample size of at least three batches, each containing a minimum of three cells per batch, was determined based on previous experience to ensure reliability of the findings.

Immunocytochemistry

Cultured hippocampal neurons were fixed for 15 min in 4% PFA. After a 10-min permeabilizing step with 0.1% Triton X-100 in PBS, the neurons were blocked in 10 mM Tris solution supplemented with 0.15 M NaCl, 0.1% Tween-20 and 4% non-fat milk powder for 1 h at room temperature (RT). The neurons were then incubated with primary antibodies (rabbit anti-CaMKII(1:1000), which was kindly provided by Prof. Kohji Fukunaga,[18] and mouse anti-GAD67 (Invitrogen Cat# MA5-24909, RRID:AB_2723202, 1:500)) overnight at 4 °C and subsequently incubated with a secondary Alex Fluor 568-conjugated goat anti-mouse antibody (Invitrogen, 1:500) combined with an Alex Fluor 647-conjugated goat anti-rabbit antibody (Invitrogen, 1:500) for 1 h at RT. After washing steps with PBS, the coverslips plated with neurons were air-dried and mounted with a mounting medium (Southern Biotech) prior to examination under microscope (Leica SP8).

Electrophysiology

Standard whole-cell patch clamp recordings were performed in ND7/23 cells and primary cultured hippocampal mouse neurons (which were visualised with a Leica DM IL LED microscope) using an Axopatch 200 B amplifier, a Digidata 1440 A digitizer and Clampex 10.2 data acquisition software.[17] For recordings in ND7/23 cells, 500 nM TTX was added to the bath solution to block all endogenous Na^+ currents. Currents were filtered at 5 kHz and digitised at 20 kHz. Borosilicate glass pipettes had resistances of 1.8–3.0 MΩ when filled with the pipette solution (in mM): 10 NaCl, 1 EGTA, 10 HEPES, 140 CsF, pH 7.3 with CsOH, osmolarity 310 mOsm/kg with mannitol). The bath solution contained (in mM): 140 NaCl, 3 KCl, 1 $MgCl_2$, 1 $CaCl_2$, 10 HEPES, 20 TEACl, 5 CsCl, 0.1 $CdCl_2$, pH 7.3 with CsOH, osmolarity 320 mOsm/kg with mannitol).

Experiments with neurons were performed in absence or presence of 500 nM TTX at RT of 21–23 °C. Transfected neurons were held at –70 mV, signals were filtered at 5 kHz and digitised at 20 kHz for voltage-clamp recordings. For current-clamp recordings,

signals were filtered at 10 kHz and sampled at 100 kHz. Borosilicate glass pipettes had resistances of 3–5 MΩ. The pipette solution contained (in mM): 5 KCl, 4 ATP-Mg, 10 phosphocreatine, 0.3 GTP-Na, 10 HEPES, 125 K-gluconate, 2 $MgCl_2$ and 10 EGTA, pH 7.2 with KOH, osmolarity 290 mOsm/kg with mannitol. The bath solution contained (in mM): 125 NaCl, 25 $NaHCO_3$, 2.5 KCl, 1 $MgCl_2$, 2 $CaCl_2$, 1.25 NaH_2PO_4, 5 HEPES, 10 Glucose, pH 7.4 with NaOH, osmolarity 305 mOsm/kg with mannitol. The liquid junction potential was not corrected.

Data recording and analysis

In ND7/23 cells, Na^+ currents were recorded by a series of 100 ms-step depolarisations from –80 to +65 mV in 5 mV increments. Current density was determined by dividing peak Na^+ currents by cell capacitance. The activation curve (conductance–voltage relationship) was derived from the current–voltage relationship obtained according to:

$$g(V) = \frac{I}{V - V_{rev}} \quad (1)$$

where g is the conductance at test potential V, I the recorded peak Na^+ current, and V_{rev} the observed Na^+ reversal potential. A standard Boltzmann function was fit to the activation curves:

$$g(V) = \frac{g_{max}}{1 + exp\left[\frac{(V - V_{1/2})}{k_v}\right]} \quad (2)$$

where g_{max} is the normalised peak conductance, $V_{1/2}$ the voltage of half-maximal activation, and k_v the slope factor. Persistent Na^+ currents were determined at the end of depolarisation pulses (75–95 ms) normalised to peak currents. For the time constant of fast inactivation, a second-order exponential function was fit to the time course of fast inactivation during the first 70 ms after onset of the depolarisation. The weight of the slower second time constant was relatively small. Only the fast time constant, τ_h, was therefore used for data presentation.

Steady-state fast inactivation was investigated using a series of 100 ms conditioning pulses of various potentials followed by a 5 ms test pulse to –10 mV, at which the peak current reflected the percentage of non-inactivated channels (for p.Asn995Asp, the test pulse was 0 mV due to the strong shift of the activation curve). A standard Boltzmann function was fit to the fast inactivation curves:

$$I(V) = \frac{I_{max}}{1 + exp\left[\frac{(V - V_{1/2})}{k_v}\right]} \quad (3)$$

where I is the recorded current amplitude at the conditioning potential V, I_{max} the maximal current amplitude, $V_{1/2}$ the voltage of half-maximal inactivation, and k_V the slope factor. Recovery from fast inactivation was recorded using a 100 ms depolarising pulse to –20 mV followed by repolarization to either –80 or –100mV with increasing time intervals and a final test pulse to –20 mV (for p.Asn995Asp, the conditioning and test pulses were 0 mV). A first-order exponential function with an initial delay was fit to the time course of recovery from inactivation, yielding the time constant τ_{rec}.

For experiments in cultured hippocampal neurons, the peak Na^+ current, passive membrane properties and action potential properties were obtained and analysed as previously described.[17] The Na^+ current and action potential firing were recorded from the same neurons, thus the other ionic currents (i.e. K^+ and Ca^{2+} currents) were not blocked. Recordings of Na^+ current in presence of TTX were only used for estimation of the Na^+ peak current amplitude to reflect the expression of transfected WT or mutant $Na_V1.6$ channels in neuronal cultures.

All data were analysed using Clampfit software of pClamp 10.6 (Axon Instruments), Microsoft Excel (Microsoft Corporation), or Graphpad prism (Graphpad software). The D'Agostino & Pearson test was used to assess normality assumption, and Bartlett's test was used to assess the homogeneity of variance. For statistical evaluation of two groups, independent t-test was applied for normally distributed and Mann–Whitney U test for not normally distributed data. For comparison of normally distributed multiple groups, ordinary ANOVA was used for the data with equal SDs, while Brown-Forsythe and Welch ANOVA was used for the data without equal SDs; For comparison of not normally distributed multiple groups, Kruskal–Wallis test was applied. All groups were analysed with Dunnett's post hoc test. For all groups with significance compared to controls, P values with two significant digits were reported; any P values less than 0.0001 were reported as "$P < 0.0001$".

Role of funding source

The funders had no role in study design, data collection, data analysis or interpretation, and decision to prepare or publish the manuscript.

Results

Variant features and clinical characteristics

In total, we recruited ten individuals from nine unrelated families (Fig. 1a). Their demographic and clinical data are summarised in Table 1. Inheritance was confirmed by segregation analysis to be *de novo* in two cases, with three cases of unknown inheritance (likely sporadic; family declined testing or was unavailable),

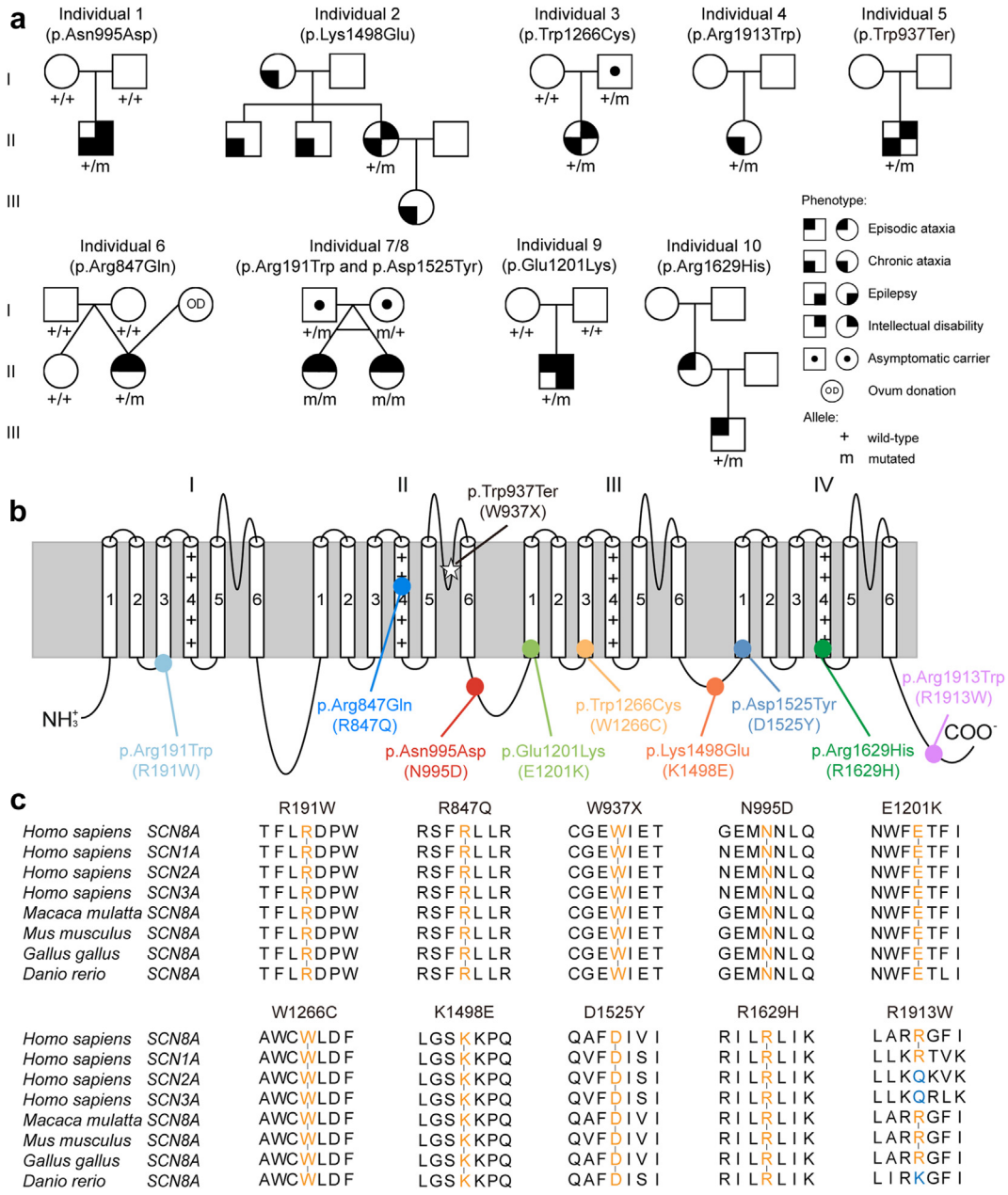

***Fig. 1: SCN8A* variants associated with episodic or chronic ataxia.** (a) Pedigrees of study participants. Empty symbols show unaffected individuals. For each individual, genetic testing results are shown where available: Alleles are shown as mutant (m), wildtype (+), or status unknown (blank). In individual 6, ovum donation (OD) resulted in dizygotic twins. Individuals 7 and 8 are monozygotic twins affected by biallelic variants. (b) Localization of variants in human $Na_v1.6$ channel. (c) Variants and their surrounding amino acids are highly evolutionarily conserved except p.Arg1913Trp.

and five familial cases (Table 1). Median length of follow-up was 11.25 [6.96–13.00] years. Clinical features other than ataxia were uncommon, with an Inventory of Non-Ataxia Signs (INAS) count of mean 1.8 (n = 6, range 1–7) (Table 1 and Supplementary Table S1).[19] Two individuals had epilepsy: Individual 1 experienced febrile seizures and typical absence seizures with generalised epileptiform discharges on EEG and an onset of 12 months, while individual 9 had drug-resistant myoclonic seizures with an onset of 8 months as well as unknown-onset impaired-awareness. Individuals 7 and 8 had electrographic abnormalities

	Individual 1	Individual 2	Individual 3	Individual 4	Individual 5	Individual 6	Individual 7	Individual 8	Individual 9	Individual 10
Family	1	2	3	4	5	6	7	7	8	9
Gender, age at last exam	M, 6 y 2 m	F, 71 y	F, 13 y	F, 55 y	M, 51 y	F, 8 y	F, 11 y 5 m	F, 11 y 5 m	M, 15 y	M, 10 y
Variant, inheritance	c.2983 A > G p.Asn995Asp de novo	c.4492 A > G p.Lys1498Glu NA	c.3798G > C p.Trp1266Cys paternal	c.5737C > T p.Arg1913Trp NA	c.2810G > A p.Trp937Ter NA	c.2540G > A p.Arg847Gln maternal	c.571C > T p.Arg191Trp and c.4573G > T p.Asp1525Tyr biparental inheritance		c.3601G > A p.Glu1201Lys de novo	c.4886G > A p.Arg1629His maternal
Ataxia syndrome	chronic ataxia	chronic ataxia	chronic ataxia	chronic ataxia	chronic ataxia	episodic ataxia	episodic ataxia	episodic ataxia	Episodic ataxia	Episodic ataxia
Ataxia onset	3 m	childhood	16 m	35 y	51 y	2 m	2 m	2 m	8 m	2 m
Development/ Cognitive	global developmental delay, mild ID	global developmental delay, mild ID	mild global developmental delay	normal	mild ID	mild global developmental delay, mild ID	mild global developmental delay, mild ID	mild global developmental delay, mild ID	global developmental delay, mild ID	normal
Epilepsy, seizure onset	GGE; 12 m	NA	NA	NA	NA	NA	NA	NA	Unclassified; 8 m	NA
Treatment	none	none	L-DOPA: no effect	none	none	none	AZA: full response; VPA: no effect; LTG: suspected worsening	AZA: full response; VPA: no effect; LTG: suspected worsening	AZA: partial response; OXC: worsening of symptoms	AZA: partial response; CBZ: worsening of symptoms

M = male; F = female; y = years; m = months; NA = not available/applicable; AZA = acetazolamide; VPA = valproic acid; LTG = lamotrigine; OXC = oxcarbazepine; CBZ = carbamazepine; ID = intellectual disability; GGE = genetic generalized epilepsy.

Table 1: **Clinical features of the individuals with disease-associated *SCN8A* variants.**

including generalised epileptiform discharges, but no evidence of seizures.

Individuals 1–5, carrying the variants p.Asn995Asp, p.Lys1498Glu, p.Trp1266Cys, p.Arg1913Trp, and p.Trp937Ter respectively, demonstrated a clinical presentation consistent with chronic progressive ataxia (Table 1 and Supplementary Table S1). Onset of gait or limb ataxia varied between birth (delayed motor milestones) and 51 years. Severity of ataxia ranged from mild to moderate (SARA scores of 2–16 points, mean 11).[20] Individual 3 was the least affected, with unlimited walking distance and difficulties only while running or climbing stairs (Supplementary Video 1). Mild intellectual disability was present in three of the five individuals (individuals 1, 2, and 5).

Individuals 6–10 had features consistent with episodic ataxia (Table 1 and Supplementary Table S1). They carried the variants p.Arg847Gln (6), p.Arg191Trp and p.Asp1525Tyr (7,8), p.Glu1201Lys (9), and p.Arg1629His (10). Except for individual 9, who had mild gait ataxia, none had interictal ataxia symptoms. None had cerebellar atrophy on magnetic resonance imaging (MRI). In all individuals, the duration of follow-up was ≥5 years with no evidence of disease progression or features of chronic ataxia. Attacks began early in life (2 months in individuals 6 and 10) and were infrequent: Individuals 6–8 reported a mean frequency of 2–3 attacks per year, individual 10 every 6–8 weeks. Individuals 6–9, mean age 12.6 years, noted attack frequency decreasing with age. All attacks were long-lasting: participants reported sudden-onset gait ataxia or dysarthria and clumsiness that persisted for at least several hours, up to 5–7 days. Individuals 6 and 10 presented with tonic upward gaze and vertical nystagmus (Supplementary Video 2). All reported triggers including fatigue, stress, fever, cold weather, or exercise.

Medical treatment was attempted in five individuals with epilepsy or episodic ataxia, as anti-seizure medication in individual 1 and 9, and empirical treatment for episodic ataxia otherwise. Individuals 7 and 8 did not benefit from combination treatment with acetazolamide and lamotrigine, but both improved substantially after discontinuation of lamotrigine. In individual 9, introduction of oxcarbazepine at a low dose (150 mg daily) led to an immediate and profound exacerbation of both interictal gait ataxia and frequency of episodic attacks. In individual 10, carbamazepine led to an increase of attack frequency and severity, but acetazolamide reduced attack frequency (from once every 3–5 weeks to once every 6–8 weeks).

Functional characterizations of *SCN8A* variants in ND7/23 cells

The ten variants investigated in this study are distributed across the entire *SCN8A* structure, and nine of them are located in highly conserved protein regions

except R1913W (Fig. 1b and c, from now on, we use the one letter code for variants for compatibility with figures). W937X is causing a premature stop codon and is highly likely to undergo nonsense-mediated decay. This variant is therefore presumed to be a LOF variant. The biophysical changes caused by the nine missense variants were examined in ND7/23 cells. Endogenous Na^+ currents were blocked using TTX. Representative Na^+ currents mediated by transfected WT or mutant channels' cDNA are shown in two clusters according to their distinct clinical phenotypes (Fig. 2a and f). Out of the four variants associated with chronic progressive ataxia, N995D, K1498E and W1266C decreased peak Na^+ current densities and caused a depolarising shift as well as a decreased slope of activation curves compared to WT (Fig. 2b and c, Table 2). Additionally, K1498E shifted the

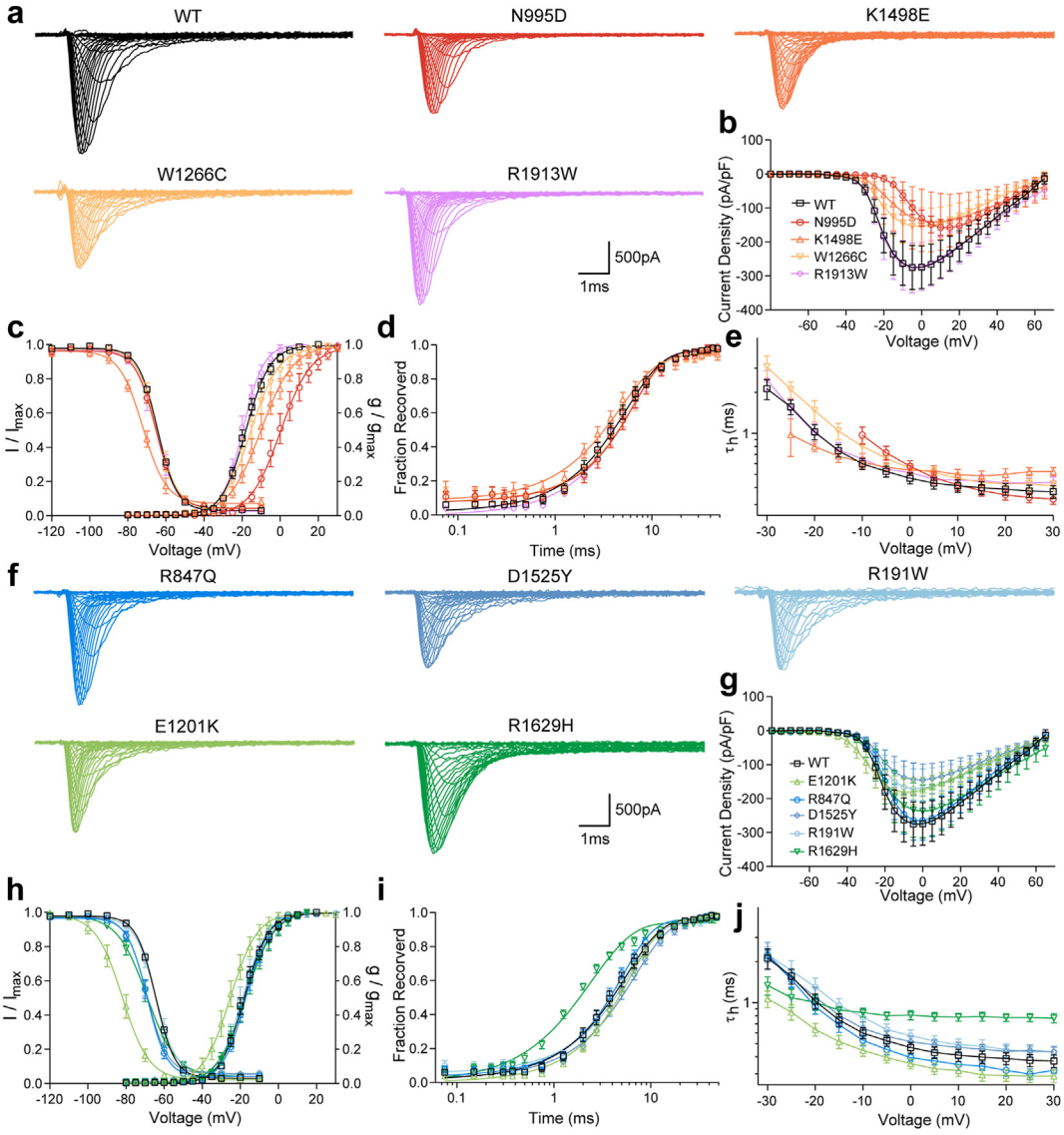

***Fig. 2:* Functional studies of *SCN8A* wild-type (WT) and variants in ND7/23 cell.** (a) Representative traces of Na^+ current for WT and variants associated with chronic ataxia. (b) Peak Na^+ currents normalised by cell capacitances were plotted versus voltage. (c) Voltage-dependent steady state activation and inactivation curves. Lines represent Boltzmann functions fit to the data points. (d) Time course of recovery from fast inactivation at −100 mV. (e) Voltage-dependence of the time constant of fast inactivation τ_h. (f) Representative traces of Na^+ current for WT and variants associated with episodic ataxia. (g) Peak Na^+ currents normalised by cell capacitances were plotted versus voltage. (h) Voltage-dependent steady state activation and inactivation curves. Lines represent Boltzmann function as in D. (i) Time course of recovery from fast inactivation at −100 mV. (j) Voltage-dependence of the time constant of fast inactivation τ_h. All data are shown as means ± 95% confidence interval. Numbers of recorded cells and statistical analysis are provided in Table 2.

	Steady-state activation			Steady-state inactivation			Trec at −100 mV, ms	n	Th at 0 mV, ms	Persistent current, % of peak current	Current density, pA/pF	n
	V ½, mV	k	n	V ½, mV	k	n						
WT	−18.1 ± 3.6	−6.1 ± 1.1	27	−64.9 ± 2.2	4.9 ± 0.33	27	4.9 ± 1.5	27	0.47 ± 0.10	0.55 ± 0.57	−250.2 [−342.1, −143.7]	27
N995D	−0.9 ± 3.5 (*P* < 0.0001)	−7.2 ± 1.0 (*P* = 0.0049)	25	−65.3 ± 2.2	4.8 ± 0.57	25	5.3 ± 1.3	10	0.50 ± 0.07	0.56 ± 0.67	−156.4 ± 59.5	25
K1498E	−9.3 ± 4.2 (*P* < 0.0001)	−8.4 ± 1.1 (*P* < 0.0001)	16	−72.3 ± 3.6 (*P* < 0.0001)	5.8 ± 1.07 (*P* < 0.0001)	16	4.1 ± 0.7	11	0.54 ± 0.08	2.05 ± 0.85 (*P* < 0.0001)	−144.3 ± 89.2 (*P* = 0.0069)	16
W1266C	−14.7 ± 4.3 (*P* = 0.0478)	−7.3 ± 1.4 (*P* = 0.0043)	16	−64.8 ± 3.2	4.9 ± 0.37	17	5.3 ± 1.7	14	0.55 ± 0.06	0.55 ± 0.60	−123.0 [−217.3, −94.8] (*P* = 0.023)	16
R1913W	−19.5 ± 2.7	−5.4 ± 1.3	15	−65.3 ± 2.7	5.2 ± 0.42	15	5.4 ± 0.9	14	0.51 ± 0.07	0.60 ± 0.48	−278.3 ± 131.7	15
R847Q	−16.8 ± 2.7	−6.1 ± 0.9	18	−69.0 ± 2.7 (*P* < 0.0001)	5.0 ± 0.40	17	4.3 ± 0.6	17	0.41 ± 0.03	0.58 ± 0.60	−268.0 ± 127.0	18
D1525Y	−17.2 ± 4.2	−6.8 ± 1.1	26	−68.9 ± 2.2 (*P* < 0.0001)	5.2 ± 0.72	20	6.1 ± 1.4	18	0.50 ± 0.08	0.72 ± 0.82	−107.1 [−187.6, −85.9] (*P* = 0.0006)	26
R191W	−17.9 ± 4.0	−6.3 ± 1.3	20	−64.4 ± 1.5	5.1 ± 0.42	19	5.1 ± 1.0	19	0.53 ± 0.08	0.53 ± 0.79	−174.7 ± 126.8 (*P* = 0.0425)	20
E1201K	−25.1 ± 4.5 (*P* < 0.0001)	−6.7 ± 0.8	16	−81.1 ± 2.8 (*P* < 0.0001)	6.6 ± 0.36 (*P* < 0.0001)	16	5.3 ± 1.0	16	0.38 ± 0.05 (*P* = 0.0004)	0.62 ± 0.75	−182.0 ± 78.1	16
R1629H	−17.1 ± 4.1	−7.1 ± 1.0 (*P* = 0.032)	17	−69.0 ± 3.8 (*P* < 0.0001)	7.4 ± 0.53 (*P* < 0.0001)	17	2.1 ± 0.5 (*P* < 0.0001)	17	0.81 ± 0.09 (*P* < 0.0001)	1.95 ± 1.05 (*P* = 0.0005)	−193.5 [−311.5, −134.5]	17

Data are presented as means ± SD for normally distributed groups, and median [IQR] for not normally distributed groups; *n* = number of recorded cells; WT = wild-type.

Table 2: **Biophysical properties of *SCN8A* WT and mutant channels recorded in ND7/23 cell.**

fast inactivation curve towards more hyperpolarized potentials, decreased its slope, and increased persistent current (Fig. 2b, Table 2). None of these three variants affected the kinetics of fast inactivation or its recovery (Fig. 2d and e). In summary, these three variants caused predominant LOF effects. We did not observe any significant biophysical changes for R1913W (Fig. 2a–e, Table 2).

Out of the five variants associated with episodic ataxia, only D1525Y and R191W decreased Na^+ current densities (Fig. 2g, Table 2). Four variants (R847Q, D1525Y, E1201K and R1629H) caused a hyperpolarizing shift of fast inactivation. E1201K and R1629H also decreased the slope of the fast inactivation curve (Fig. 2h, Table 2). E1201K caused a hyperpolarizing shift of the activation curve and accelerated the time course of fast inactivation (Fig. 2g and j, Table 2). R1629H accelerated recovery from fast inactivation, markedly slowed fast inactivation, and increased the persistent current (Fig. 2i and j, Table 2). Considering that R191W and D1525Y represent biallelic variants, we conducted co-transfections of these two variants using a 1:1 ratio (2 µg R191W + 2 µg D1525Y) into ND7/23 cells, aiming to assess their physiological impact. Our observations revealed a hyperpolarizing shift in fast inactivation (Supplementary Fig. S1 and Supplementary Table S2). Overall, R847Q, D1525Y, and R191W showed LOF effects, whereas E1201K and R1629H caused mixed GOF and LOF effects.

Taken together, three variants associated with chronic progressive ataxia caused predominant LOF effects mainly by shifting the activation curve towards more depolarised potentials as well as decreasing Na^+ current densities. One variant did not cause any biophysical changes. Conversely, 4/5 variants associated with episodic ataxia caused a hyperpolarizing shift of fast inactivation, and 2/5 variants decreased Na^+ current densities, accompanied by other changes in gating properties. The functional consequences of two variants causing episodic ataxia, E1201K and R1629H, as well as a chronic ataxia-related variant without biophysical alterations, R1913W, were further examined in primary neuronal cultures to delineate their effect on action potential firing.

Studies of three variants in cultured hippocampal neurons

The effects of E1201K, R1629H and R1913W were examined in both excitatory and inhibitory neurons. TTX-resistant *SCN8A* WT or mutant constructs were transfected into primary neuronal cultures together with GFP under either the CaMKII or Dlx promoter to target either excitatory or inhibitory neurons. Immunocytochemical studies showed that Dlx-GFP positive neurons were stained by the inhibitory neuronal biomarker GAD67 but not by excitatory neuronal biomarker CaMKII, vice versa for CaMKII-GFP positive neurons, confirming correctly labelled neuronal populations for our recordings (Fig. 3a). We first conducted experiments in transfected neurons in the absence of TTX. Under these conditions, endogenous and transfected Na^+ channels jointly determine action potential firing. A series of current injections ranging from −50 to 300 pA elicited action potential firing and representative raw

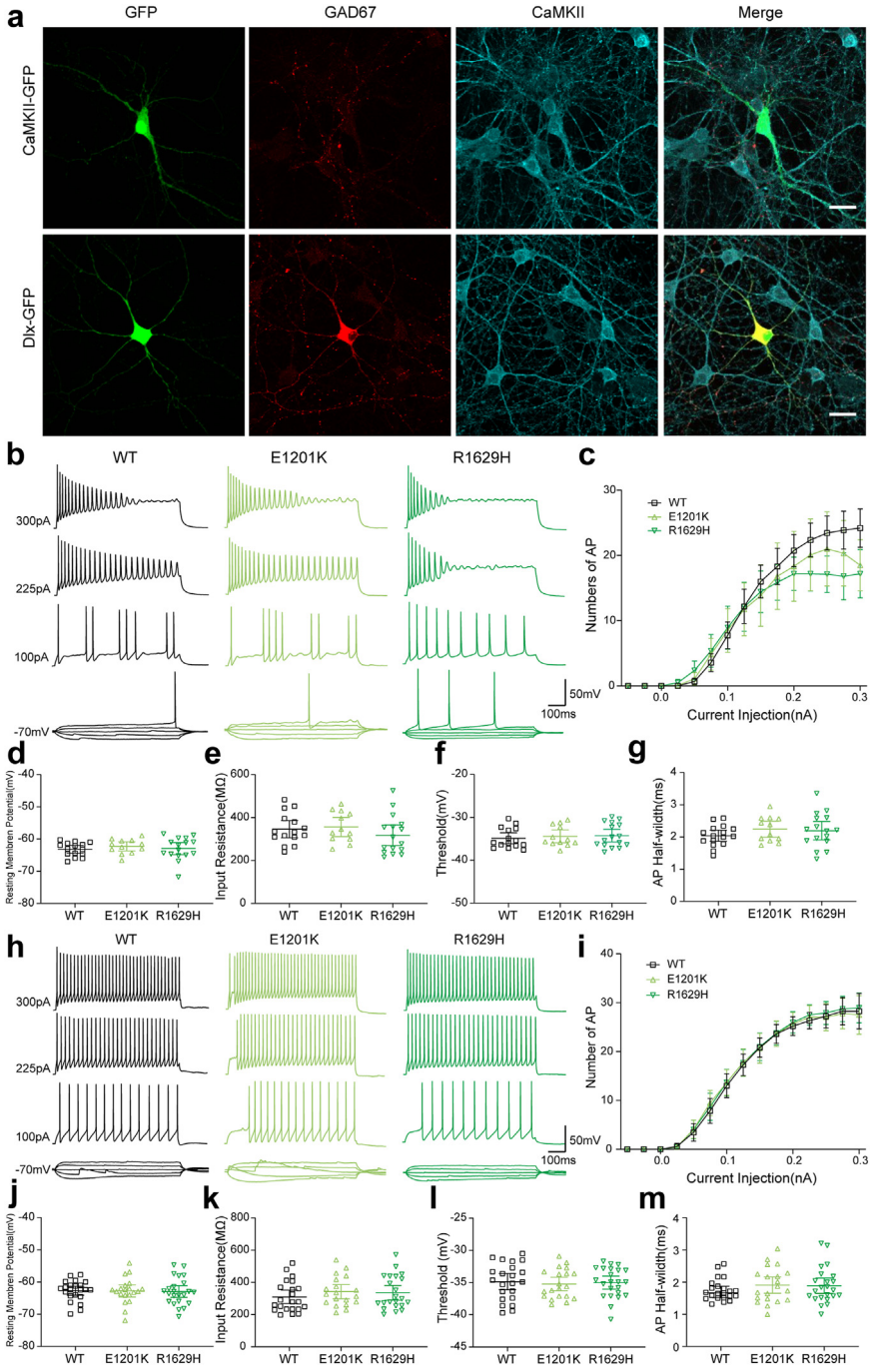

Fig. 3: **Intrinsic neuronal and firing properties of cultured hippocampal excitatory and inhibitory neurons transfected with *SCN8A* WT or mutant channels in absence of TTX.** (a) Transfected hippocampal neurons indicated by CaMKII- or Dlx-GFP (green) were stained with a monoclonal anti-GAD67 antibody (red) and a monoclonal anti-CaMKII antibody (cyan). Scale bar: 20 μm. (b) Representative firing traces of evoked action potentials (APs) recorded in hippocampal excitatory neurons transfected with WT, p.Glu1201Lys (E1201K) or p.Arg1629His (R1629H), respectively. (c) Number of APs plotted versus injected current. WT, *n* = 16; E1201K, *n* = 12; R1629H, *n* = 16. (d) Resting membrane potential and (e) Input resistance of transfected excitatory neurons. (f) Threshold of first evoked AP. (g) Half-width of single AP. (h) Representative firing traces of evoked APs recorded in transfected hippocampal inhibitory neurons. (i) Number of APs plotted versus injected current. WT, *n* = 23; E1201K, *n* = 20; R1629H, *n* = 22. (j) Resting membrane potential and (k) Input resistance of transfected inhibitory neurons. (l) Threshold of first evoked AP. (m) Half-width of single AP. All data are presented as means ± 95% confidence interval. Detailed statistical analysis is provided in Table 3.

	Resting membrane potential (RMP), mV	Input resistance, MΩ	Action potential parameters			Rheobase, pA	I/O area under the curve, nA	n
			Peak amplitude, mV	Half-width, ms	Threshold, mV			
WT-excitatory	−63.2 ± 2.1	346 ± 72	125.2 ± 7.7	2.04 ± 0.32	−34.9 ± 2.3	65.6 ± 15.5	4.03 ± 1.1	16
E1201K-excitatory	−62.3 ± 2.2	356 ± 71	118.4 ± 6.9	2.24 ± 0.39	−34.4 ± 2.4	60.4 ± 27.1	3.65 ± 1.7	12
R1629H-excitatory	−63.0 ± 3.5	318 ± 91	127.6 ± 7.3	2.19 ± 0.54	−34.3 ± 2.8	65.6 ± 37.5	3.41 ± 0.9	16
WT-inhibitory	−62.7 ± 3.2	309 ± 95	118.7 ± 10.3	1.76 ± 0.33	−34.9 ± 2.8	55.7 ± 23.1	5.19 ± 1.1	22
E1201K-inhibitory	−62.8 ± 4.0	342 ± 91	117.0 ± 14.0	1.91 ± 0.55	−35.2 ± 2.3	51.3 ± 19.0	5.45 ± 1.3	20
R1629H-inhibitory	−63.0 ± 4.2	335 ± 104	119.1 ± 13.0	1.89 ± 0.56	−35.0 ± 2.3	54.6 ± 22.7	5.34 ± 1.3	23

I/O = input–output curve. Data are presented as means ± SD for normally distributed groups; n = number of recorded cells. WT = wild-type.

Table 3: **Intrinsic neuronal properties and single potential parameters in transfected excitatory or inhibitory hippocampal neurons in the absence of TTX.**

traces are shown in Fig. 3b and h. Analysis of the area under the input–output relationship of WT and two mutant channels showed no significant difference in neuronal firing in both excitatory and inhibitory neurons (Table 3). The other neuronal properties (e.g., resting membrane potential, input resistance, and parameters of single action potentials) were also comparable between WT and two mutant channels (Fig. 3c–g and i–m, Table 3).

We then examined the neuronal intrinsic and firing properties in transfected neurons in the presence of TTX blocking endogenous Na^+ channels, so that neuronal firing was mediated only by transfected channels. Representative traces of TTX-resistant sodium current were shown Supplementary Fig. S2. In excitatory neurons, though only few action potentials can be elicited in neurons transfected with WT channels, the action potential firing frequency was reduced for E1201K, and increased for R1629H (Fig. 4a–c) without significant changes of passive membrane properties (Fig. 4d–f). Analysis of single action potentials indicated that both variants decreased the action potential amplitude (Fig. 4g and i). Furthermore, E1201K decreased the threshold to elicit an action potential, which is consistent with the hyperpolarizing shift of activation caused by this variant in ND7/23 cells (Fig. 4g and h), whereas R1629H increased the action potential half-width (Fig. 4j) consistent with the slowing of fast inactivation and increased persistent current. R1913W did not affect action potential firing in either excitatory or inhibitory neurons in the presence of TTX (Supplementary Fig. S3).

In inhibitory neurons, both variants decreased action potential firing frequency, as indicated by representative raw traces and analysis of the area under the curve of input–output relationships (Fig. 4k–m). Particularly, E1201K decreased the peak Na^+ current amplitude in transfected neurons compared to WT, which contributed to an increased input resistance and scarce action potential firing in the presence of TTX (Fig. 4n and p). Hence, no parameters of single action potentials could be obtained for this variant. As in excitatory neurons, R1629H decreased amplitude and increased half-width of single action potentials in inhibitory neurons (Fig. 4q–t). In summary, E1201K decreased neuronal firing in both excitatory and inhibitory neurons in the presence of TTX showing predominant LOF effects, whereas R1629H enhanced neuronal firing in excitatory neurons and decreased neuronal firing in inhibitory neurons showing distinct effects on different types of neurons.

Discussion

We identified ten variants in *SCN8A* in ten individuals affected by a spectrum of hereditary ataxia syndromes, including episodic and chronic ataxia with and without additional symptoms. Four variants associated with chronic progressive ataxia caused strong LOF by a depolarising shift of activation and decreased Na^+ current density (N995D, K1498E, W1266C), or through predicted haploinsufficiency (W937X). Three variants associated with episodic ataxia caused LOF by a hyperpolarizing shift of fast inactivation (R847Q and D1525Y) or decreased Na^+ current density (R191W and D1525Y). Two episodic ataxia variants, E1201K and R1629H, caused gain- and loss-of function effects on molecular/channel level, but significantly decreased neuronal firing in inhibitory neurons showing a predominant LOF effect. The functional consequences caused by these variants thus nicely correlate with the clinical severity, indicating that (i) strong LOF effects were observed for variants associated with chronic ataxia, most notably for N995D, which was found to be associated with the most severe phenotype, (ii) milder LOF effects were observed for variants associated with episodic ataxia than those in chronic ataxia. No functional changes were observed for one variant (R1913W, located in the distal C-terminal which is the least conserved domain among human sodium channels) in both neuroblastoma cells and neuronal cultures, indicating that another, yet unknown (e.g., genetic or acquired) defect is responsible for the chronic ataxia in this patient.

Dozens of years after movement disorders had been observed in several spontaneous *Scn8a* mouse lines (e.g.

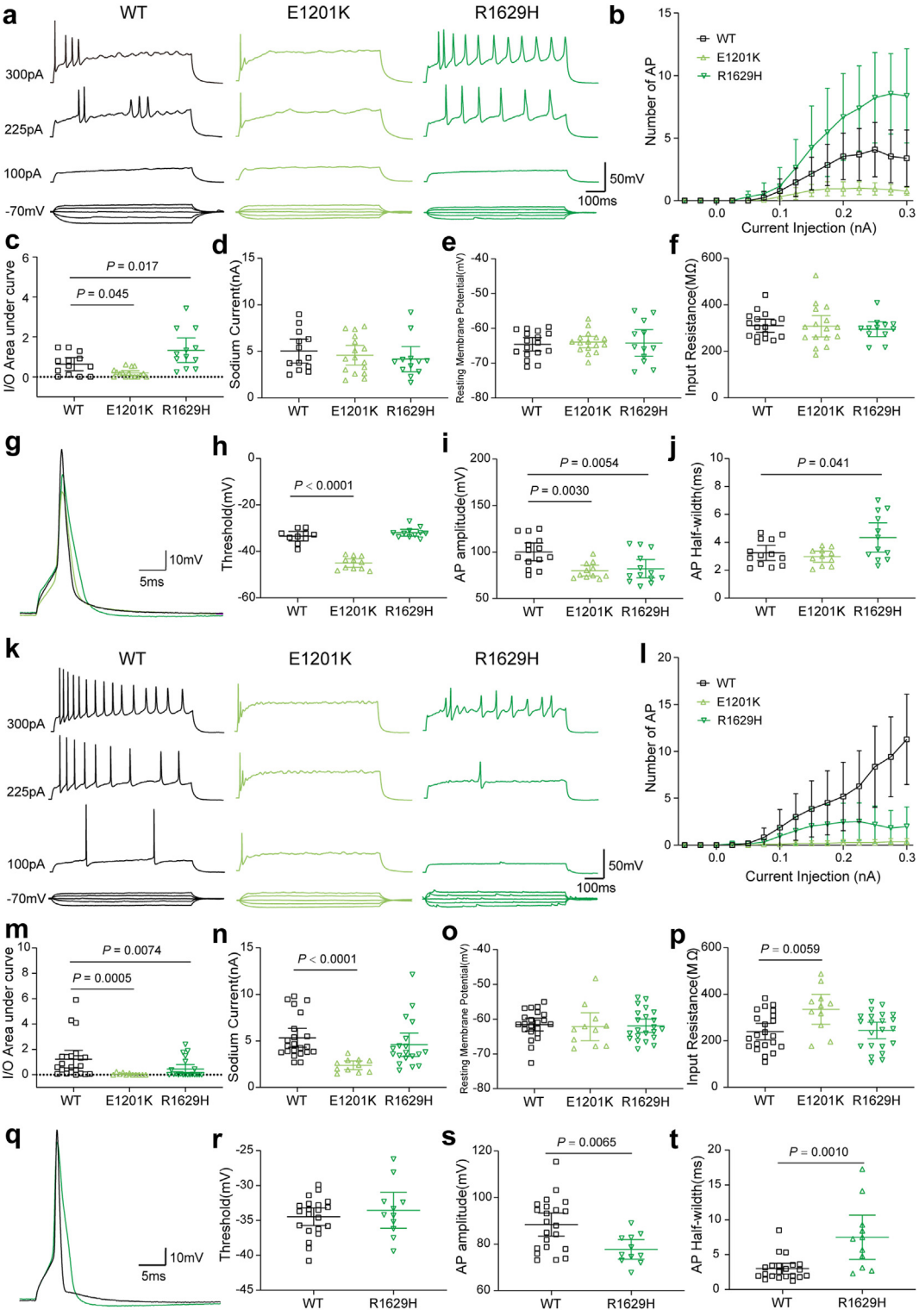

Fig. 4: **Intrinsic neuronal and firing properties of cultured hippocampal excitatory and inhibitory neurons transfected with *SCN8A* WT or mutant channels in presence of TTX.** (a) Representative firing traces of evoked action potentials (APs) recorded in hippocampal excitatory neurons transfected with WT, p.Glu1201Lys (E1201K) or p.Arg1629His (R1629H) respectively. (b) Number of APs plotted versus injected current. WT, *n* = 13; E1201K, *n* = 16; R1629H, *n* = 12. (c) Area under the curve (AUC) for the input–output relationships. E1201K decreased and

	Sodium current, pA	Resting membrane potential (RMP), mV	Input resistance, MΩ	Action potential parameters			I/O area under the curve, nA	n
				Peak amplitude, mV	Half-width, ms	Threshold, mV		
WT-excitatory	5033 ± 2125	−64.6 ± 3.8	310 ± 55	100.2 ± 16.6	3.24 ± 0.91	−33.5 ± 2.9	0.63 ± 0.55	13
E1201K-excitatory	4591 ± 1985	−64.0 ± 3.1	307 ± 86	79.9 ± 8.7 (P = 0.003)	2.97 ± 0.59	−45.0 ± 2.8 (P < 0.0001)	0.19 ± 0.21 (P = 0.045)	16
R1629H-excitatory	3886 [2872, 4197]	−64.2 ± 6.0	294 ± 50	82.0 ± 16.3 (P = 0.0054)	4.34 ± 1.65 (P = 0.041)	−32.0 ± 2.2	1.33 ± 0.97 (P = 0.017)	12
WT-inhibitory	4413 [1795, 6738]	−61.6 ± 4.1	239 ± 80	88.4 ± 11.2	2.55 [1.90, 3.49]	−34.5 ± 2.8	0.64 [0.09, 1.43]	22
E1201K-inhibitory	2374 ± 712 (P < 0.0001)	−62.2 ± 6.0	335 ± 96 (P = 0.0059)	–	–	–	0.05 ± 0.09 (P = 0.0005)	11
R1629H-inhibitory	3746 [3138, 5234]	−61.9 ± 4.4	244 ± 80	77.7 ± 6.3 (P = 0.0065)	7.49 ± 4.72 (P = 0.001)	−33.6 ± 3.8	0.01 [0.00, 0.74] (P = 0.0074)	22

Inhibitory neurons transfected with E1201K mutant channels barely exhibit action potential firing upon current injection, hence no parameters for single action potential were listed. I/O = input–output curve. Data are presented as means ± SD for normally distributed groups, and median [IQR] for not normally distributed groups; n = number of recorded cells; WT = wild-type.

Table 4: **Intrinsic neuronal properties and single potential parameters in transfected excitatory or inhibitory hippocampal neurons in the presence of TTX.**

Scn8a med, *Scn8a* med^{j} and *Scn8a* jolting),[21] ataxia as a clinical feature of *SCN8A*-associated disorders has been recognized.[6,22,23] In 2006, Trudeau et al. screened 151 individuals with familial or sporadic ataxia and identified an individual with a variant in *SCN8A* (p.Pro1719Argfs*6) leading to a LOF by truncating the C terminal domain, which was associated with early-onset severe chronic ataxia and cerebellar atrophy.[24] In our previous large study of *SCN8A*-associated disorders in ~400 individuals, ataxia was present in 11/136 individuals with GOF variants, and 5/34 individuals with LOF variants.[8] Ataxia as an accompanying symptom may thus develop as a consequence of both GOF- and LOF-causing variants, but a predominant ataxia phenotype seems to be the consequence of a LOF of $Na_V1.6$. In our study, we observed only one single case of *SCN8A*-related ataxia in a continuous series of about 1200 index patients who attended the ataxia clinic in Tübingen since 2012 and received a comprehensive genetic work-up including *SCN8A* by ataxia gene panel, exome or genome sequencing. The prevalence of such variants is thus considered to be very low.

Previously, Wengert et al. reported two families with biallelic *SCN8A* variants (G269R/T1360R and G822R/R1638C) including compound-heterozygous individuals where one allele caused almost complete abolishment of Na^+ current, while the other allele caused LOF gating effects (shift of activation or fast inactivation curves), resulting in severe DEE.[25] The heterozygous parents exhibited mild cognitive deficits. In the present study, we identified a pair of monozygotic twins with biallelic *SCN8A* variants, R191W (which decreased Na^+ current density) and D1525Y (which caused a decreased current density as well as a hyperpolarizing shift of fast inactivation). However, the heterozygous parents were not affected (Fig. 1a and Table 1). This may indicate that R191W and D1525Y caused milder LOF effects than the two biallelic DEE variants reported by Wengert et al., resulting in milder phenotypes.

Thus far, previous and our current studies have identified around 40 LOF variants in *SCN8A*, which have been shown to be causative for a wide spectrum of neuronal disorders, including intellectual disability without epilepsy, generalised (absence) epilepsy, severe DEE, and now chronic and episodic ataxia. Since a large proportion of missense variants showing almost no Na^+ current and nonsense variants caused diverse neuronal disorders covering almost the whole spectrum mentioned above, it is difficult to establish a correlation between clinical severity and electrophysiological

R1629H increased AUC compared with WT. (d) Peak Na^+ current amplitudes, (e) Resting membrane potential and (f) Input resistance of transfected excitatory neurons. (g) Representative traces of evoked single AP for WT and mutant channels recorded in transfected excitatory neurons. E1201K and R1629H decreased single AP amplitude (i), E1201K decreased threshold (h), and R1629H increased half-width(j) of single APs. (k) Representative firing traces of evoked APs recorded in hippocampal inhibitory neurons transfected with WT, E1201K and R1629H, respectively. (l) Number of APs plotted versus injected current. WT, n = 22; E1201K, n = 11; R1629H, n = 19. (m) Both variants decreased AUC of the input–output relationships compared with WT. (n) E1201K decreased peak Na^+ current amplitudes, which is consistent with the increased input resistance (p) observed in transfected inhibitory neurons. (o) Resting membrane potential of inhibitory neurons transfected with WT or mutant channels. (q) Representative firing traces of evoked single action potential for WT and R1629H recorded in transfected inhibitory neurons. R1629H didn't affect AP threshold(r), but decreased AP amplitude(s) and increased AP half-width (t). All data are presented as means ± 95% confidence interval. One-way ANOVA with Dunnett's post hoc test or ANOVA on ranks with Dunn's post hoc test were performed. Detailed statistical analysis is provided in Table 4.

properties of *SCN8A* LOF variants as we did for *SCN8A* GOF variants,[8] although it appears that episodic ataxia variants caused milder LOF effects than chronic ataxia variants as well as the biallelic *SCN8A* variants causing DEE. Previously, it has been found in mouse models that *Gabra2* splice variants can modify the severity of epileptic phenotypes caused by *SCN8A* GOF variants.[26,27] The pleiotropy of LOF variants may be due to yet unknown modifying factors which should be further explored. It is likely that some degree of this phenotypic variability is related to environmental or other unknown factors that we cannot easily account for by our experimental results, as has been demonstrated for other sodium channelopathies.[28,29]

Since $Na_V1.6$ channels are expressed in the cell bodies and dendrites of Purkinje neurons and contribute to around 40% of all components of Na^+ currents,[30] *SCN8A* LOF variants may result in a decreased inhibitory output of Purkinje neurons as the common underlying molecular and cellular mechanisms for *SCN8A*-related episodic and chronic ataxia. Reduced inhibitory output of Purkinje neurons underlies the common pathophysiological mechanism of ataxia associated with variants in other voltage-gated cation channels.[31] Global deletion of $Na_V1.1$ channels directly decreased the firing rate of Purkinje neurons causing ataxia.[30] LOF variants in *KCNA1* encoding the $K_V1.1$ channel resulted in an enhancement of GABAergic inhibition on Purkinje neurons reducing their spontaneous firing leading to episodic ataxia.[32] Variants in other voltage-gated cation channels such as $K_V1.2$, $K_V3.3$, $Ca_V2.1$, and $Ca_V3.1$ channels directly or through parallel-fibre/climbing-fibre pathway indirectly decreased Purkinje neuronal function, causing episodic and chronic ataxia.[33–36] Several mouse models carrying *SCN8A* LOF variants showed ataxia phenotypes and decreased firing rates of Purkinje neurons.[15,37] Interestingly, selective removal of *SCN8A* in Purkinje neurons but not in granule neurons decreased firing rate of Purkinje neurons causing mild ataxia, and double deletion of *SCN8A* in both Purkinje and granule neurons further decreased Purkinje neuronal firing leading to severe ataxia.[38] These previous findings thus support that *SCN8A* LOF variants characterised in the current study may directly decrease the excitability of Purkinje neurons with different severity resulting in episodic and chronic ataxia. It is not clear why a few *SCN8A* GOF variants caused ataxia as an accompanying symptom of epilepsy. Due to the broad expression of *SCN8A* in both excitatory and inhibitory neurons in the brain,[39] these GOF variants may indirectly affect the output of Purkinje neurons through unknown neuronal circuits contributing to ataxia.

Similar phenotypes are known in other voltage-gated sodium channel disorders. In *SCN2A*, episodic ataxia has been described in 21 individuals, with a third affected by the recurring gain-of-function variant A263V. In their study, neonatal-onset seizures were common (6/7 individuals) and some response to acetazolamide was seen in 3/9 individuals at a dose of 4.3–30 mg/kg body weight/day. Age at onset of episodic ataxia was late, between 18 and 36 months, with attacks ranging from short daily events up to 1–2 episodes per year, each lasting several weeks.[40] This syndrome is now recognized as episodic ataxia type 9 (MIM #618924). In *SCN1A*, chronic ataxia has long been acknowledged as a comorbidity of Dravet syndrome, generally as part of the characteristic motor phenotype including 'crouch gait'.[30,41–43] More recently, Choi et al. reported *SCN1A*-related episodic ataxia in 2/28 individuals.[44] With our report, three major neuronal voltage-gated sodium channel genes (*SCN1A, SCN2A,* and *SCN8A*) have now been implicated as causative genes of episodic ataxia.

Our findings highlight the importance of the concept of paralog variants and investigations in neurons to elucidate differential effects on channel function. Consistent with our observations in ND7/23 cells, the paralog variant of E1201K in *SCN2A*, E1211K, caused hyperpolarizing shifts of both activation and fast inactivation curves in HEK293 cells.[45] This variant was previously observed in an individual with a phenotype consistent with *SCN2A*-LOF-related epilepsy.[16,45] Despite the distinct expression patterns and roles of *SCN2A* and *SCN8A* in brain, our neuronal results confirmed a LOF mechanism for this variant in both *SCN2A* and *SCN8A* genes causing similar phenotypes. The paralog variant of R1629H in *SCN1A*, R1648H, which has been associated with febrile and afebrile seizures in humans, caused GOF and LOF effects in tsA201 cells and reduced neuronal firing in mouse inhibitory neurons (similar to our results).[46] The corresponding variant in the mouse *SCN8A* gene, R1627H, increased seizure susceptibility and reduced motor function.[47] R1627H also decreased action potential firing in hippocampal inhibitory neurons but increased action potential firing in hippocampal pyramidal neurons, consistent with our own neuronal results.[48] Taken together, our results indicate (i) neuronal investigations are essential to disentangle the functional consequences of variants, particularly for those variants causing both GOF and LOF effects; (ii) paralog variants in Na_V channels may share similar molecular/cellular mechanisms, favouring the approach of predicting and validating functional effects by considering the effects of similar variants in paralog genes[48]; (iii) variants may cause distinct effects in different types of neurons, i.e. excitatory and inhibitory neurons, thus leading to diverse phenotypes. The reasons for this observation remain elusive; different compositions of ion channels may explain that, but would need additional investigations. It will be also of interest to further explore the effects of these variants in Purkinje and granule cells to better understand the pathophysiological mechanisms in the cerebellum.

Considering potential therapeutic approaches for *SCN8A*-related episodic or chronic ataxia, we note that all variants presented here resulted in an overall LOF effect. Sodium channel blockers are a standard treatment in episodic ataxia type 1.[49] In our cohort, we found this approach to be harmful to four individuals. This is expected, as the use of sodium channel blockers in individuals with LOF variants in voltage-gated sodium channels can enhance channel dysfunction and should be avoided.[50] Thus, identifying *SCN8A* variants as pathogenic in individuals with hereditary ataxia may guide treatment and reduce potential harm. However, our studies are not clinical trials and we did not test treatment effects. Care should be taken when our results are used for guiding diagnosis and treatment of *SCN8A*-related ataxia.

In summary, all variants characterised in this study showed predominant LOF effects, and chronic ataxia variants caused stronger LOF effects than episodic ataxia variants. These LOF variants may result in a decreased firing frequency of Purkinje cells as the common underlying molecular and cellular mechanisms for *SCN8A*-related episodic and chronic progressive ataxia. This fits nicely with the observation that sodium channel blockers worsen symptoms in four individuals with episodic ataxia. Our findings thus expand the clinical spectrum of *SCN8A*-related neuronal disorders and confirm *SCN8A* as a gene associated with predominant chronic or episodic ataxia.

Contributors

Conception and design of the study: YL, HaL, CMB, HoL, RSM, KJ. Acquisition and analysis of data: HaL, CMB, YL, RSM, KJ, JDOE, SAA, DGNN, TL, EG, HVR, RR, CB, GH, EB, NG, DO, AT, MK, EIG, LS, ZF, HoL. Drafting a significant portion of the manuscript or figures: CMB, HaL, YL, HoL. CMB, HaL and YL directly accessed and verified the data reported in the manuscript. All authors have read and approved the final version of the manuscript.

Data sharing statement

All detailed clinical data are available in supplementary table. Functional research data in this work paper will be made available from the lead contact upon any reasonable request from qualified investigators.

Declaration of interests

MK reports a doctoral grant from DAAD. JDOE is coordinator of the Chorea and Huntington Disease Group (ERN-RND). EB has received funding from the Dutch Epilepsy Foundation, on behalf of the Dravet syndrome Foundation Netherlands/Flanders, the JANIVO foundation and the K.F. Hein Foundation. LS declares grants from the German Research Foundation, German Ministry of Heath, European Commission, and Innovationsfond, and has received consulting fees from Vico Therapeutics and Novartis. RSM has received consulting and speaker fees from UCB and Orion and speaker fees from EISAI and Angelini Pharma. All other authors report no competing interests.

Acknowledgements

We thank the affected individuals and their families for participating in this study.

We acknowledge support from the Open Access Publication Fund of the University of Tübingen.

Appendix A. Supplementary data

Supplementary data related to this article can be found at https://doi.org/10.1016/j.ebiom.2023.104855.

References

1 Klockgether T, Paulson H. Milestones in ataxia. *Mov Disord*. 2011;26(6):1134–1141.
2 Schule R, Schols L. [Ataxias and hereditary spastic paraplegias]. *Nervenarzt*. 2017;88(7):720–727.
3 Jen JC, Graves TD, Hess EJ, et al. Primary episodic ataxias: diagnosis, pathogenesis and treatment. *Brain*. 2007;130(Pt 10):2484–2493.
4 Hadjivassiliou M, Martindale J, Shanmugarajah P, et al. Causes of progressive cerebellar ataxia: prospective evaluation of 1500 patients. *J Neurol Neurosurg Psychiatry*. 2017;88(4):301–309.
5 Bushart DD, Shakkottai VG. Ion channel dysfunction in cerebellar ataxia. *Neurosci Lett*. 2019;688:41–48.
6 Meisler MH, Hill SF, Yu W. Sodium channelopathies in neurodevelopmental disorders. *Nat Rev Neurosci*. 2021;22(3):152–166.
7 Mantegazza M, Cestèle S, Catterall WA. Sodium channelopathies of skeletal muscle and brain. *Physiol Rev*. 2021;101(4):1633–1689.
8 Johannesen KM, Liu Y, Koko M, et al. Genotype-phenotype correlations in *SCN8A*-related disorders reveal prognostic and therapeutic implications. *Brain*. 2022;145(9):2991–3009.
9 Gardella E, Moller RS. Phenotypic and genetic spectrum of *SCN8A*-related disorders, treatment options, and outcomes. *Epilepsia*. 2019;60(Suppl 3):S77–S85.
10 Durr A. Autosomal dominant cerebellar ataxias: polyglutamine expansions and beyond. *Lancet Neurol*. 2010;9(9):885–894.
11 Requena T, Espinosa-Sanchez JM, Lopez-Escamez JA. Genetics of dizziness: cerebellar and vestibular disorders. *Curr Opin Neurol*. 2014;27(1):98–104.
12 Helbig KL, Hedrich UB, Shinde DN, et al. A recurrent mutation in *KCNA2* as a novel cause of hereditary spastic paraplegia and ataxia. *Ann Neurol*. 2016;80(4):638–642.
13 Burk K, Kaiser FJ, Tennstedt S, et al. A novel missense mutation in *CACNA1A* evaluated by in silico protein modeling is associated with non-episodic spinocerebellar ataxia with slow progression. *Eur J Med Genet*. 2014;57(5):207–211.
14 Kohrman DC, Smith MR, Goldin AL, et al. A missense mutation in the sodium channel *Scn8a* is responsible for cerebellar ataxia in the mouse mutant jolting. *J Neurosci*. 1996;16(19):5993–5999.
15 Wolff M, Johannesen KM, Hedrich UBS, et al. Genetic and phenotypic heterogeneity suggest therapeutic implications in *SCN2A*-related disorders. *Brain*. 2017;140(5):1316–1336.
16 Kohler S, Gargano M, Matentzoglu N, et al. The human phenotype ontology in 2021. *Nucleic Acids Res*. 2021;49(D1):D1207–D1217.
17 Liu Y, Schubert J, Sonnenberg L, et al. Neuronal mechanisms of mutations in *SCN8A* causing epilepsy or intellectual disability. *Brain*. 2019;142(2):376–390.
18 Fukunaga K, Goto S, Miyamoto E. Immunohistochemical localization of Ca^{2+}/calmodulin-dependent protein kinase II in rat brain and various tissues. *J Neurochem*. 1988;51(4):1070–1078.
19 Jacobi H, Rakowicz M, Rola R, et al. Inventory of Non-Ataxia Signs (INAS): validation of a new clinical assessment instrument. *Cerebellum*. 2013;12(3):418–428.
20 Schmitz-Hubsch T, du Montcel ST, Baliko L, et al. Scale for the assessment and rating of ataxia: development of a new clinical scale. *Neurology*. 2006;66(11):1717–1720.
21 Meisler MH, Plummer NW, Burgess DL, Buchner DA, Sprunger LK. Allelic mutations of the sodium channel *SCN8A* reveal multiple cellular and physiological functions. *Genetica*. 2004;122:37–45.
22 Woodruff-Pak DS, Green JT, Levin SI, Meisler MH. Inactivation of sodium channel *Scn8A* (Na-sub(v)1.6) in Purkinje neurons impairs learning in Morris water maze and delay but not trace eyeblink classical conditioning. *Behav Neurosci*. 2006;120(2):229–240.
23 Burgess DL, Kohrman DC, Galt J, et al. Mutation of a new sodium channel gene, *Scn8a*, in the mouse mutant "motor endplate disease." *Nat Genet*. 1995;10(4):461–465.
24 Trudeau MM, Dalton JC, Day JW, et al. Heterozygosity for a protein truncation mutation of sodium channel *SCN8A* in a patient with cerebellar atrophy, ataxia, and mental retardation. *J Med Genet*. 2006;43(6):527–530.

25 Wengert ER, Tronhjem CE, Wagnon JL, et al. Biallelic inherited *SCN8A* variants, a rare cause of *SCN8A*-related developmental and epileptic encephalopathy. *Epilepsia*. 2019;60(11):2277–2285.
26 Yu W, Hill SF, Xenakis JG, et al. *Gabra2* is a genetic modifier of Scn8a encephalopathy in the mouse. *Epilepsia*. 2020;61(12):2847–2856.
27 Yu W, Mulligan MK, Williams RW, Meisler MH. Correction of the hypomorphic *Gabra2* splice site variant in mouse strain C57BL/6J modifies the severity of *Scn8a* encephalopathy. *HGG Adv*. 2021;3(1):100064.
28 Martins Custodio H, Clayton LM, Bellampalli R, et al. Widespread genomic influences on phenotype in Dravet syndrome, a 'monogenic'condition. *Brain*. 2023;146(9):3885–3897.
29 Skotte L, Fadista J, Bybjerg-Grauholm J, et al. Genome-wide association study of febrile seizures implicates fever response and neuronal excitability genes. *Brain*. 2022;145(2):555–568.
30 Kalume F, Yu FH, Westenbroek RE, et al. Reduced sodium current in Purkinje neurons from Nav1.1 mutant mice: implications for ataxia in severe myoclonic epilepsy in infancy. *J Neurosci*. 2007;27(41):11065–11074.
31 Hoxha E, Balbo I, Miniaci MC, Tempia F. Purkinje cell signaling deficits in animal models of ataxia. *Front Synaptic Neurosci*. 2018;10:6.
32 Lauxmann S, Sonnenberg L, Koch NA, et al. Therapeutic potential of sodium channel blockers as a targeted therapy approach in *KCNA1*-associated episodic ataxia and a comprehensive review of the literature. *Front Neurol*. 2021;12:703970.
33 Xie G, Harrison J, Clapcote SJ, et al. A new Kv1.2 channelopathy underlying cerebellar ataxia. *J Biol Chem*. 2010;285(42):32160–32173.
34 Pietrobon D. CaV2.1 channelopathies. *Pflugers Arch*. 2010;460(2):375–393.
35 Hashiguchi S, Doi H, Kunii M, et al. Ataxic phenotype with altered CaV3.1 channel property in a mouse model for spinocerebellar ataxia 42. *Neurobiol Dis*. 2019;130:104516.
36 Irie T, Matsuzaki Y, Sekino Y, Hirai H. Kv3.3 channels harbouring a mutation of spinocerebellar ataxia type 13 alter excitability and induce cell death in cultured cerebellar Purkinje cells. *J Physiol*. 2014;592(1):229–247.
37 Raman IM, Sprunger LK, Meisler MH, Bean BP. Altered subthreshold sodium currents and disrupted firing patterns in Purkinje neurons of Scn8a mutant mice. *Neuron*. 1997;19(4):881–891.
38 Levin SI, Khaliq ZM, Aman TK, et al. Impaired motor function in mice with cell-specific knockout of sodium channel *Scn8a* (Nav1.6) in cerebellar purkinje neurons and granule cells. *J Neurophysiol*. 2006;96(2):785–793.
39 Vacher H, Mohapatra DP, Trimmer JS. Localization and targeting of voltage-dependent ion channels in mammalian central neurons. *Physiol Rev*. 2008;88(4):1407–1447.
40 Schwarz N, Bast T, Gaily E, et al. Clinical and genetic spectrum of *SCN2A*-associated episodic ataxia. *Eur J Paediatr Neurol*. 2019;23(3):438–447.
41 Catterall WA. Dravet syndrome: a sodium channel interneuronopathy. *Curr Opin Physiol*. 2018;2:42–50.
42 Wolff M, Casse-Perrot C, Dravet C. Severe myoclonic epilepsy of infants (Dravet syndrome): natural history and neuropsychological findings. *Epilepsia*. 2006;47(Suppl 2):45–48.
43 Aljaafari D, Fasano A, Nascimento FA, et al. Adult motor phenotype differentiates Dravet syndrome from Lennox-Gastaut syndrome and links *SCN1A* to early onset parkinsonian features. *Epilepsia*. 2017;58(3):e44–e48.
44 Choi KD, Kim JS, Kim HJ, et al. Genetic variants associated with episodic ataxia in korea. *Sci Rep*. 2017;7(1):13855.
45 Ogiwara I, Ito K, Sawaishi Y, et al. De novo mutations of voltage-gated sodium channel alphaII gene *SCN2A* in intractable epilepsies. *Neurology*. 2009;73(13):1046–1053.
46 Hedrich UB, Liautard C, Kirschenbaum D, et al. Impaired action potential initiation in GABAergic interneurons causes hyperexcitable networks in an epileptic mouse model carrying a human Na(V)1.1 mutation. *J Neurosci*. 2014;34(45):14874–14889.
47 Makinson CD, Dutt K, Lin F, et al. An Scn1a epilepsy mutation in *Scn8a* alters seizure susceptibility and behavior. *Exp Neurol*. 2016;275(Pt 1):46–58.
48 Brünger T, Pérez-Palma E, Montanucci L, et al. Conserved patterns across ion channels correlate with variant pathogenicity and clinical phenotypes. *Brain*. 2022;146(3):923–934.
49 Orsucci D, Raglione LM, Mazzoni M, Vista M. Therapy of episodic ataxias: case report and review of the literature. *Drugs Context*. 2019;8:212576.
50 Wirrell EC, Laux L, Donner E, et al. Optimizing the diagnosis and management of dravet syndrome: recommendations from a north american consensus panel. *Pediatr Neurol*. 2017;68:18–34.e3.